

UCSF

UC San Francisco Previously Published Works

Title

Cutting Edge: IL-6-Driven Immune Dysregulation Is Strictly Dependent on IL-6R α -Chain Expression.

Permalink

<https://escholarship.org/uc/item/1vn994n9>

Journal

Journal of immunology (Baltimore, Md. : 1950), 204(4)

ISSN

0022-1767

Authors

Mufazalov, Ilgiz A
Andruszewski, David
Schelmbauer, Carsten
et al.

Publication Date

2020-02-01

DOI

10.4049/jimmunol.1900876

Peer reviewed



Cutting Edge: IL-6–Driven Immune Dysregulation Is Strictly Dependent on IL-6R α -Chain Expression

This information is current as of February 13, 2020.

Ilgiz A. Mufazalov, David Andruszewski, Carsten Schelmbauer, Sylvia Heink, Michaela Blanfeld, Joumana Masri, Yilang Tang, Rebecca Schöler, Christina Eich, F. Thomas Wunderlich, Susanne H. Karbach, Jeffrey A. Bluestone, Thomas Korn and Ari Waisman

J Immunol 2020; 204:747-751; Prepublished online 10 January 2020;

doi: 10.4049/jimmunol.1900876

<http://www.jimmunol.org/content/204/4/747>

Supplementary Material <http://www.jimmunol.org/content/suppl/2020/01/09/jimmunol.1900876.DCSupplemental>

References This article **cites 22 articles**, 8 of which you can access for free at: <http://www.jimmunol.org/content/204/4/747.full#ref-list-1>

Why *The JI*? Submit online.

- **Rapid Reviews! 30 days*** from submission to initial decision
- **No Triage!** Every submission reviewed by practicing scientists
- **Fast Publication!** 4 weeks from acceptance to publication

**average*

Subscription Information about subscribing to *The Journal of Immunology* is online at: <http://jimmunol.org/subscription>

Permissions Submit copyright permission requests at: <http://www.aai.org/About/Publications/JI/copyright.html>

Email Alerts Receive free email-alerts when new articles cite this article. Sign up at: <http://jimmunol.org/alerts>



Cutting Edge: IL-6–Driven Immune Dysregulation Is Strictly Dependent on IL-6R α -Chain Expression

Ilgiz A. Mufazalov,^{*,†} David Andruszewski,^{*} Carsten Schelmbauer,^{*} Sylvia Heink,[‡] Michaela Blanfeld,^{*} Joumana Masri,^{*} Yilang Tang,^{*} Rebecca Schöler,^{*,§,¶} Christina Eich,^{*} F. Thomas Wunderlich,^{||,#} Susanne H. Karbach,^{*,§,¶} Jeffrey A. Bluestone,[†] Thomas Korn,^{‡,***,1} and Ari Waisman^{*,1}

IL-6 binds to the IL-6R α -chain (IL-6R α) and signals via the signal transducer gp130. Recently, IL-6 was found to also bind to the cell surface glycoprotein CD5, which would then engage gp130 in the absence of IL-6R α . However, the biological relevance of this alternative pathway is under debate. In this study, we developed a mouse model, in which murine IL-6 is overexpressed in a CD11c–Cre–dependent manner. Transgenic mice developed a lethal immune dysregulation syndrome with increased numbers of Ly-6G⁺ neutrophils and Ly-6C^{hi} monocytes/macrophages. IL-6 overexpression promoted activation of CD4⁺ T cells while suppressing CD5⁺ B-1a cell development. However, additional ablation of IL-6R α protected IL-6–overexpressing mice from IL-6–triggered inflammation and fully phenocopied IL-6R α –deficient mice without IL-6 overexpression. Mechanistically, IL-6R α deficiency completely prevented downstream activation of STAT3 in response to IL-6. Altogether, our data clarify that IL-6R α is the only biologically relevant receptor for IL-6 in mice. *The Journal of Immunology*, 2020, 204: 747–751.

Elevated levels of IL-6 have been observed in numerous pathological conditions, and several drugs are successfully used in a series of human diseases, including rheumatoid arthritis, Castleman disease, and giant cell arteritis

to target IL-6 and its receptor, IL-6R α -chain (IL-6R α) (1). For other diseases like multiple myeloma and neuromyelitis optica, the clinical program for the development of IL-6–neutralizing agents is very advanced, and drugs targeting IL-6 or IL-6R α might be licensed for these diseases in the near future (2).

IL-6, together with IL-11, IL-27, CNTF, LIF, OSM, CT-1, and CLC, belongs to the group of cytokines that use gp130 for signal transduction (3). Since its discovery in 1990, it was believed that the IL-6–signaling complex consists of a unique IL-6–binding receptor IL-6R α (also known as CD126) and the signal transducer gp130 (4). The assembly of IL-6, IL-6R α , and gp130 leads to activation of STAT3-mediated intracellular signaling pathways, which control cell survival, activation, and proliferation (2). IL-6R α also exists in a soluble form, which is generated via secretion or shedding of membrane-bound IL-6R α . The complex of IL-6 and soluble IL-6R α is able to bind to gp130 and then induce STAT3 phosphorylation in cells that do not express IL-6R α themselves. This signaling modality of IL-6 was termed IL-6 *trans*-signaling (5). A third modality of IL-6 signaling, called IL-6 cluster signaling, is mediated by cell-bound presentation of the IL-6/IL-6R α complex in *trans* by a donor cell to a receiving cell that expresses gp130 (2, 6). In both IL-6 *trans*-signaling and IL-6 cluster signaling, cells that express gp130, but lack IL-6R α , still respond to IL-6.

In 2016, an alternative pathway of IL-6 signal transduction was proposed in which IL-6 binds to the membrane-anchored

^{*}Institute for Molecular Medicine, University Medical Center of the Johannes Gutenberg-University Mainz, 55131 Mainz, Germany; [†]Diabetes Center, University of California, San Francisco, CA 94143; [‡]Abteilung für Experimentelle Neuroimmunologie, Klinikum rechts der Isar, Technische Universität München, 81675 Munich, Germany; [§]Center for Cardiology, University Medical Center of the Johannes Gutenberg-University Mainz, 55131 Mainz, Germany; [¶]Center for Thrombosis and Hemostasis, University Medical Center of the Johannes Gutenberg-University Mainz, 55131 Mainz, Germany; ^{||}Max Planck Institute for Metabolism Research, Cologne Cluster of Excellence in Aging-Associated Diseases, Institute for Genetics, 50931 Cologne, Germany; [#]Center for Molecular Medicine Cologne, Institute for Genetics, University of Cologne, 50931 Cologne, Germany; and ^{***}Munich Cluster for Systems Neurology, SyNergy, 81377 Munich, Germany

¹T.K. and A.W. coshared authorship.

ORCID: 0000-0001-9332-0131 (I.A.M.); 0000-0003-3645-1877 (D.A.); 0000-0001-5764-9642 (C.S.); 0000-0001-7560-8369 (Y.T.); 0000-0002-2460-6512 (R.S.); 0000-0002-4414-9048 (C.E.); 0000-0003-4462-3747 (S.H.K.); 0000-0001-8793-7848 (J.A.B.); 0000-0002-3633-0955 (T.K.); 0000-0003-4304-8234 (A.W.).

Received for publication July 29, 2019. Accepted for publication December 15, 2019.

This work was supported by the Deutsche Forschungsgemeinschaft (DFG) (TRR128-A07 [to A.W. and T.K.]). In addition, T.K. was supported by the DFG Grant SFB1054-B06 and the Munich Cluster for Systems Neurology as well as by the European Research Council (CoG 647215) and the Federal Ministry of Education and Research (01G11605B). A.W. was, in addition, supported by the DFG Grants WA1600/10-1

and TRR128-A03. S.H.K. was supported by the Margarethe Waitz-Foundation, the DFG Grant KA4035/1-1, by the Boehringer Ingelheim Foundation “Novel and Neglected Cardiovascular Risk Factors: Molecular Mechanisms and Therapeutic Implications,” and by the German Center of Cardiovascular Research (Deutsches Zentrum für Herz-Kreislauf-Forschung) “Platelet Signatures and Psoriasis in Cardiac Dysfunction.” S.H.K. was also supported by the Federal Ministry of Education and Research (BMBF 01EO1503), related to this study. I.A.M. and J.A.B. were supported by the Sean N. Parker Autoimmunity Research Laboratory.

I.A.M. designed the experiments, analyzed the data, and wrote the manuscript; D.A., C.S., S.H., M.B., Y.T., and C.E. performed experiments; S.H.K., J.M., and R.S. generated conditional IL-6 transgenic mice; F.T.W. contributed essential reagents; J.A.B. critically reviewed and edited the manuscript; T.K. and A.W. designed the experiments, wrote the manuscript, and supervised the study.

Address correspondence and reprint requests to Dr. Ilgiz A. Mufazalov, Institute for Molecular Medicine, Building 308A, Room 1.204, Langenbeckstrasse 1, 55131 Mainz, Germany. E-mail address: ilgiz.mufazalov@uni-mainz.de

The online version of this article contains supplemental material.

Abbreviations used in this article: DC, dendritic cell; IL-6R α , IL-6R α -chain; OE, overexpression; VD[−], viability dye–negative.

Copyright © 2020 by The American Association of Immunologists, Inc. 0022-1767/20/\$37.50

glycoprotein CD5 instead of IL-6R α and, via gp130, initiates STAT3 phosphorylation in B cells (7). This study suggested the CD5-dependent pathway of IL-6 signaling was critical in the promotion of cancer progression (7). However, the mechanism for this novel IL-6 binding was not elucidated. In fact, soluble CD5, despite binding to IL-6, is unable to induce IL-6 *trans*-signaling (8). Massive overproduction of IL-6 is observed in sepsis (9) and has been reported during the cytokine release syndrome in response to CAR-T cell immune therapies (10). To keep exaggerated IL-6 responses in check, any design of therapeutic intervention needs to consider potential alternative signaling pathways of IL-6. In particular, the idea of CD5 as a molecule to substitute for IL-6R α in forming the IL-6 signal transduction complex might be relevant in this context.

To test whether IL-6R α can be functionally replaced in any IL-6–signaling modality, we used a set of genetically modified mice with IL-6 overexpression. High levels of IL-6 led to systemic inflammation, which subsequently resulted in a lethal outcome. In contrast, mice that overexpressed IL-6, but lacked IL-6R α , did not show STAT3 phosphorylation and were completely protected from IL-6–mediated pathology, suggesting that IL-6R α is indispensable for IL-6 signaling.

Materials and Methods

Mice

Mice with conditional *Il6ra* allele (*Il6ra* flox) (11) and CD11c-Cre mice (12) have been previously described. IL-6R α full-knockout (*Il6ra*^{−/−}) mice were selected from the breeding between *Il6ra* flox mice and CD11c-Cre mice, which displayed occasional spontaneous germline Cre activity. Principles used to generate mice with the knock-in of a transgene into *Rosa26* locus have been previously described (13). Details of the generation of mice carrying murine cDNA in the CAG–(loxP)STOP(loxp)–IL-6–IRES–eGFP transgene inserted in the *Rosa26* locus will be reported elsewhere. For breeding strategies involving IL-6 overexpression and mouse group abbreviations, refer to Supplemental Fig. 1A. All mice were on C57BL/6 background and were bred in-house under specific pathogen-free conditions. For experiments, 5–9-wk-old, gender-matched mice were used in accordance with the guidelines of the central animal facility institution (Translational Animal Research Center, University of Mainz).

Mouse sample collection

Single-cell suspensions from spleen and lymph nodes were prepared by mechanical dissociation in PBS supplemented with 2% FCS. Peritoneal lavage was performed on lethally anesthetized mice with 5 ml of PBS supplemented with 3% FCS. Peripheral blood was collected from the tail vein. RBCs were removed using ACK lysis buffer.

IL-6 ELISA

A murine IL-6 ELISA Kit (BD Biosciences) was used to analyze IL-6 levels in the blood serum. Plates were measured with the Infinite M200 PRO NanoQuant reader (Tecan).

Flow cytometry

Single-cell suspensions were stained with Abs together with viability dyes (Supplemental Table I). Stained cells were acquired on FACSCanto II (BD Biosciences), and data were analyzed with FlowJo software. Gating strategy always considered cell size, excluded duplets, and defined living cells as viability dye–negative (VD[−]) population.

p-STAT3 detection by flow cytometry

Peritoneal lavage preparations pooled from four to five mice per genotype were FACS sorted for CD4[−]F4/80[−]CD19⁺CD5[−] cells and for CD4[−]F4/80[−]CD19⁺CD5⁺ cells, using FACS Aria III (BD Biosciences). Splenocytes pooled from four to five mice per genotype were FACS sorted for CD19[−]CD4⁺CD5⁺ cells. Sorted cells from *Il6ra*^{−/−} mice (CD45.2) were mixed at 1:1 ratio with wild-type *Il6ra*^{+/+} cells (CD45.1) in U-button, 96-well plates (total amount of 1.0×10^6 cells), rested for 1 h in 200 μ l of complete DMEM medium at 37°C, and stimulated with 50 ng/ml human IL-6 (Miltenyi Biotec) or 125 ng/ml of human IL-6/IL-6R α complex (hyper-IL-6, kindly provided by the group of Dr. Rose-John,

Kiel, Germany), which represents an equimolar amount as compared with the condition with soluble IL-6 only. Samples were fixed (Phosflow Lyse/Fix Buffer 5 \times ; BD Biosciences) and permeabilized (Phosflow Perm Buffer III; BD Biosciences) according to the manufacturer's recommendations. Afterwards, cells were stained with CD45.2-BV650, CD45.1-FITC, and p-STAT3(Y705)-PE FACS Abs in PBS supplemented with 2% FCS. Stained cells were acquired on a CytoFLEX flow cytometer (Beckman Coulter) and analyzed with FlowJo software.

Immunoblotting

CD19⁺ B cells and CD4⁺ T cells were isolated using MACS technology (Miltenyi Biotec) from pooled spleen and lymph node preparations. For stimulation, $(0.4\text{--}8.0) \times 10^6$ cells pooled from individual mice (three to four per genotype) were incubated in 100 μ l of complete RPMI medium at 37°C in the presence of recombinant murine IL-6 (PromoKine) and, afterward, were lysed in radioimmunoprecipitation assay buffer. Lysates were separated by SDS-PAGE (NuPAGE; Invitrogen) and transferred to polyvinylidene difluoride membranes (MilliporeSigma). Protein blots were probed with anti-phosphotyrosine 705 STAT3, anti-total STAT3 (Cell Signaling), and anti- β -actin (Sigma-Aldrich). For detection, goat anti-rabbit (Santa Cruz Biotechnology) IgG-HRP–linked secondary Abs were used.

Statistical analysis

Statistical analysis and graphical representation were performed with Prism 5 software (GraphPad). Statistical significance was calculated using the unpaired two-tailed *t* test and Gehan–Breslow–Wilcoxon test for Kaplan–Meier survival curves. The *p* values < 0.05, < 0.01, and < 0.001 were marked as *, **, and ***, respectively.

Results and Discussion

The cytokine IL-6 uses various signaling modalities (i.e., classic signaling, *trans*-signaling, and cluster signaling [also called *trans*-presentation]) (2) and might even signal through an alternative receptor complex composed of CD5 and gp130 (7). To assess the signaling modality of IL-6 under conditions of exaggerated IL-6 production, we created a murine system of sterile IL-6 overexpression *in vivo*. To this end, we generated mice carrying a CAG–(loxP)STOP(loxp)–IL-6–IRES–eGFP construct in the *Rosa26* locus. Next, we used dendritic cell (DC)–directed CD11c-Cre transgenic mice (12) to activate IL-6 overexpression (OE) from a single copy of our *Il6* transgene in mice on an IL-6R α –sufficient background (IL-6^{DC-OE} *Il6ra*^{+/+} and IL-6^{DC-OE} *Il6ra*^{+/-} [i.e., IL-6^{DC-OE}]) and on an IL-6R α –deficient background (IL-6^{DC-OE} *Il6ra*^{−/−}). As further controls, we used IL-6R α –sufficient (control) and IL-6R α –deficient (*Il6ra*^{−/−}) mice without IL-6 overexpression (Supplemental Fig. 1A).

To directly assess IL-6 overexpression, we measured IL-6 levels in the serum of 5–6-wk-old mutant mice. As expected, both groups of mice with IL-6 overexpression showed elevated levels of IL-6 in comparison with wild-type controls and *Il6ra*^{−/−} mice (Fig. 1A). IL-6 levels were significantly higher in IL-6^{DC-OE} mice than in IL-6^{DC-OE} *Il6ra*^{−/−} mice, suggesting a positive feed-forward loop for IL-6 expression in mice sufficient for IL-6R α . Mechanistically, transgenic IL-6 can promote IL-6 expression in IL-6^{DC-OE} mice, from the endogenous *Il6* locus, which remained responsive to its natural regulation. In addition, IL-6 forms a complex with the soluble IL-6R α and gp130 in the blood, which can prolong its half-life only in IL-6R α –sufficient, but not in IL-6R α –deficient, mice (14, 15).

To analyze cellular sources of transgenic IL-6, we assessed eGFP reporter expression driven by the CAG promoter after CD11c-Cre mediated excision of the *loxP* flanked STOP cassette. As expected, we found eGFP expression in DCs in IL-6^{DC-OE} and IL-6^{DC-OE} *Il6ra*^{−/−} mice (Fig. 1B, Supplemental

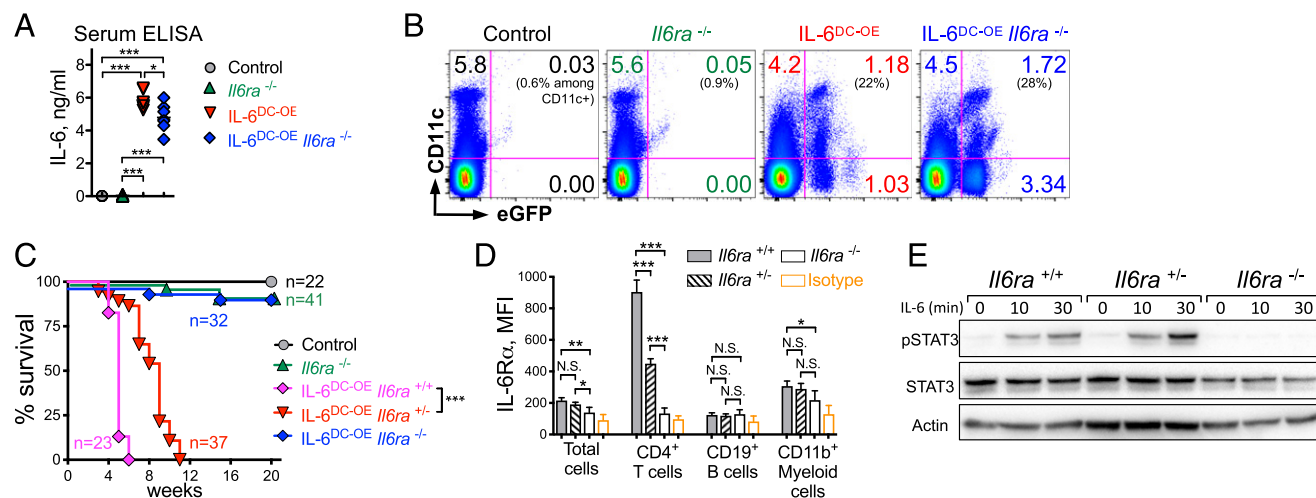


FIGURE 1. IL-6R α -dependent mortality of mice with IL-6 overexpression. **(A)** IL-6 levels in the blood serum of mice measured by ELISA. Dot plot graph shows values for individual mice and mean per group. **(B)** CD11c-Cre-mediated IL-6 overexpression reported by eGFP coexpression in DCs in the spleen. Data depict representative FACS plots with average frequencies per group. Three to four mice per group were used. For full gating strategy, refer to Supplemental Fig. 1B. **(C)** Kaplan-Meier curves depict survival of the indicated mouse strains. **(D)** Median fluorescence intensity (MFI) of the IL-6R α expression on splenocytes. Bar diagram shows mean per group \pm SD. Isotype control was stained on corresponding cell populations isolated from *Il6ra*^{+/+} mice. Four mice per group were used. For representative IL-6R α FACS staining, refer to Supplemental Fig. 2A. **(E)** Western blot analysis of STAT3 phosphorylation in response to IL-6 stimulation in vitro (10 ng/ml) of total splenocytes. Two-tailed unpaired *t* test was used for (A) and (D); Gehan-Breslow-Wilcoxon test was used for (C). All experiments were performed two to three times with similar results. **p* < 0.05, ***p* < 0.01, ****p* < 0.001.

Fig. 1C). Because of leakiness of the CD11c-Cre recombinase expression (16), we also noted limited reporter expression in other myeloid cells and in T and B cells of these mice (Supplemental Fig. 1C).

High systemic levels of IL-6 ultimately led to the death of *IL-6*^{DC-OE} mice in an IL-6R α -dependent manner (Fig. 1C). IL-6-overexpressing mice carrying both copies of *Il6ra* died within 6 wk of age, whereas deletion of one *Il6ra* allele (with one *Il6ra* allele intact in heterozygous *Il6ra*^{+/-} mice) extended the survival of *IL-6*^{DC-OE} mice until 11 wk of age. Strikingly, null deficiency in *Il6ra* restored the survival of *IL-6*^{DC-OE} *Il6ra*^{-/-} mice with IL-6 overexpression and, thus, fully rescued the phenotype of *IL-6*^{DC-OE} mice. Of note, 3 out of 41 *Il6ra*^{-/-} mice died during the observation period presumably because of their immunodeficiency (17), irrespective of IL-6 overexpression.

To study the impact of IL-6R α expression on IL-6 signaling, we isolated splenocytes from wild-type (*Il6ra*^{+/+}), *Il6ra*^{+/-}, and *Il6ra*^{-/-} mice. We observed a robust IL-6R α expression on CD4⁺ T cells and, to a lesser extent, on CD11b⁺ myeloid cells, but very limited expression on CD19⁺ B cells in wild-type mice (Fig. 1D). Deletion of a single *Il6ra* allele led to reduction in IL-6R α expression, suggesting a haploinsufficient gene dose effect (Fig. 1D), which, together with reduced frequencies of IL-6R α -positive cells in *Il6ra*^{+/-} mice (Supplemental Fig. 2A), may contribute to the reduced mortality of *IL-6*^{DC-OE} *Il6ra*^{+/-} mice in comparison with *IL-6*^{DC-OE} *Il6ra*^{+/+} mice (Fig. 1C). To determine the consequence of the lack of IL-6R α in downstream signaling events, we stimulated total splenocytes isolated from *Il6ra*^{+/+}, *Il6ra*^{+/-}, and *Il6ra*^{-/-} mice with IL-6 and assessed their STAT3 phosphorylation. We observed STAT3 phosphorylation only in wild-type and *Il6ra* heterozygous cells, whereas *Il6ra*^{-/-} splenocytes were unresponsive to stimulation with soluble IL-6 (Fig. 1E, Supplemental Fig. 2B). FACS-sorted CD5⁻ and CD5⁺ B cells, as well as CD5⁺ T cells, isolated from *Il6ra*^{-/-} mice did not respond to

soluble IL-6 either, whereas their wild-type counterparts showed a clear STAT3 activation in response to soluble IL-6 (Supplemental Fig. 2C). In contrast, IL-6R α -deficient B cells (regardless of CD5 expression), and IL-6R α -deficient T cells responded to IL-6 in the presence of exogenous IL-6R α in the form of hyper-IL-6, which represents IL-6/IL-6R α fusion protein (Supplemental Fig. 2C). These data indicate that *Il6ra*^{-/-} cells retain the ability to respond to IL-6 *trans*-signaling, whereas IL-6R α expression on the cell surface is nonredundant for classic IL-6 signaling. Together, this refutes the concept that alternative receptor molecules can compensate for the lack of IL-6R α expression.

As a consequence of IL-6 overexpression, CD11b⁺ myeloid cells massively infiltrated secondary lymphoid organs, resulting in splenomegaly of IL-6R α -sufficient *IL-6*^{DC-OE} mice (Supplemental Fig. 3). The most dramatic increase in response to transgenic IL-6 was observed in Ly-6G⁺ neutrophils and Ly-6C^{hi} monocytes/macrophages (Fig. 2A). Notably, the systemic increase in these myeloid cell subsets was completely abrogated in *IL-6*^{DC-OE} *Il6ra*^{-/-} mice lacking IL-6R α . It is likely that the systemic inflammatory response in *IL-6*^{DC-OE} mice is dependent on the massive expansion of myeloid cells.

Initially, IL-6 was named "B cell hybridoma growth factor," to acknowledge its stimulatory function on B cells (18). Although we did not detect robust expression of IL-6R α on the surface of B cells (Fig. 1D), IL-6 can pair with soluble IL-6R α and act on B cells expressing gp130. Importantly, a recent study suggested that IL-6 can bind to CD5 on B cells and activate STAT3 independently of IL-6R α (7). Among B cells, CD5 expression is rather restricted to B-1a cells, identifying this subset as a primary target for the IL-6-CD5-signaling module (19). Of note, mice with IL-6 overexpression on an IL-6R α -sufficient background exhibited a dramatic reduction in B-1a cells in the spleen (Fig. 2B), whereas IL-6R α deficiency completely prevented the IL-6-triggered loss of B-1a cells in *IL-6*^{DC-OE} *Il6ra*^{-/-} mice (Fig. 2B).

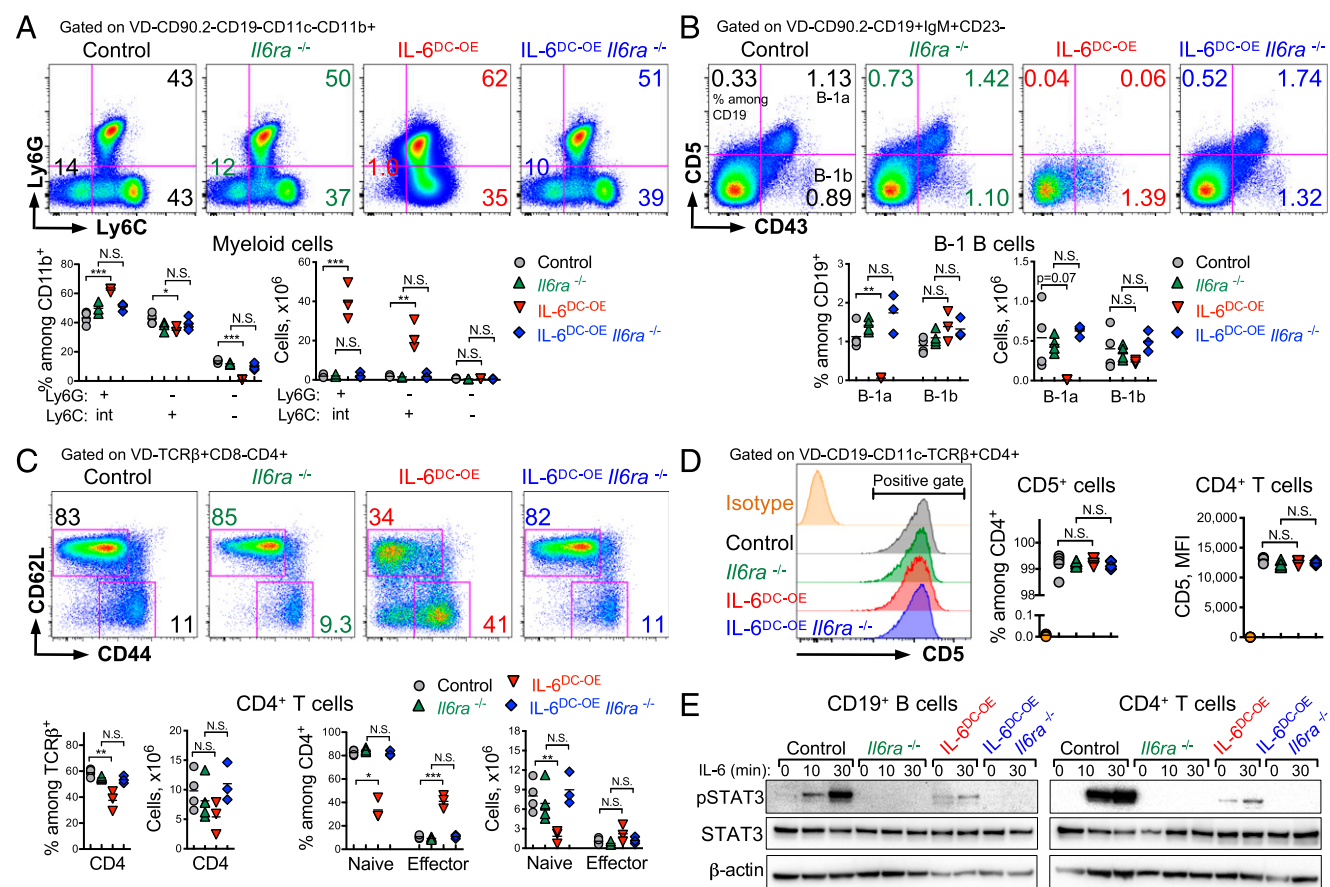


FIGURE 2. IL-6 overexpression in mice leads to increased numbers of CD11b⁺ cells and affects the composition of the B and T cell compartment. **(A)** Fractions and absolute numbers of neutrophils (Ly-6G⁺) and monocytes (Ly-6C⁺) in the spleen of the indicated mouse strains. **(B)** Fractions and absolute numbers of B-1a cells (defined as VD⁻CD90.2⁻CD19⁺IgM⁺CD23⁻CD5⁺CD43⁺ cells) and B-1b cells (defined as VD⁻CD90.2⁻CD19⁺IgM⁺CD23⁻CD5⁻CD43⁺ cells) in the spleen of the indicated mouse strains. **(C)** Fractions and absolute numbers of naive (CD44⁺CD62L^{high}) and effector (CD44⁺CD62L^{low}) CD4⁺ T cells in the spleen of the indicated mouse strains. **(D)** FACS analysis of CD5 expression on CD4⁺ T cells in the spleen of the indicated mouse strains. Data depict representative FACS histograms with the definition of CD5-positive cells. Dot plot graphs depict mean fluorescence intensity (MFI) of CD5 expression and isotype control for individual mice and mean per group. **(E)** Western blot analysis of STAT3 phosphorylation in response to IL-6 overexpression in vivo and to IL-6 stimulation in vitro (100 ng/ml) in CD19⁺ B cells and CD4⁺ T cells. Data (A–C) depict representative FACS plots with average frequencies per group. Dot plot graph shows values for individual mice and mean per group. Three to four mice per group were used. Two-tailed unpaired *t* test was used for (A)–(D). All experiments were performed two to three times with similar results. **p* < 0.05, ***p* < 0.01, ****p* < 0.001.

Because CD4⁺ T cells expressed high levels of IL-6R α (Fig. 1D), we analyzed the T cell compartment in mice with activated IL-6 pathway. We noted a significant shift toward CD44⁺CD62L^{low} effector CD4⁺ T cells in the spleen of IL-6^{DC-OE} mice in comparison with the other groups tested (Fig. 2C). However, the frequencies of effector CD4⁺ T cells in response to exaggerated IL-6 expression became normal again after IL-6R α deletion. In accordance with a previous report (20), we found abundant CD5 expression on CD4⁺ T cells, however, irrespective of their IL-6R α status (Fig. 2D).

To test STAT3 activation in specific lymphocyte subsets in mice with IL-6 overexpression, we performed immunoblotting with lysates from CD19⁺ B cells and CD4⁺ T cells. Both cell types isolated from IL-6^{DC-OE} mice displayed STAT3 phosphorylation already in steady state without additional in vitro IL-6 stimulation (Fig. 2E). Importantly, the steady-state STAT3 phosphorylation (and also STAT3 phosphorylation in response to exogenous IL-6 stimulation in vitro) was absolutely dependent on the presence of at least one copy of *Il6ra* in CD19⁺ B cells and in CD4⁺ T cells (Fig. 2E).

In the current study, we observed a lethal immunopathology in mice that overexpressed IL-6 as long as they were kept on an

IL-6R α -sufficient background. Among several genetic models with IL-6 overexpression (reviewed in Ref. 21), we activated murine IL-6 overexpression driven by CAG promoter in a CD11c-Cre-dependent manner. By genetic ablation of *Il6ra*, the phenotype of profound immune dysregulation in mice with transgenic IL-6 was completely rescued. This argues against the biological significance of any IL-6 signaling systems that would be independent of IL-6R α . In our model, we cannot draw a definite conclusion as to which IL-6 signaling modality (i.e., classic IL-6 signaling, IL-6 *trans*-signaling, or IL-6 cluster signaling [*trans*-presentation]), is the most relevant IL-6-signaling modality for the fatal immune dysregulation in IL-6^{DC-OE} mice. All three signaling modalities depend on IL-6R α , either on the side of the receiving cell (classic IL-6 signaling) or on the side of the donating cell in a soluble manner (IL-6 *trans*-signaling) or in a cell-bound manner (IL-6 *trans*-presentation) (2, 6). In steady state, CD4⁺ T cells and CD11b⁺ myeloid cells express relatively high levels of the membrane-bound IL-6R α . Thus, we speculate that, at least initially, IL-6 overexpression is operational in lymphocytes and myeloid cells through classic IL-6 signaling. The massive expansion of granulocytes in IL-6^{DC-OE} mice was a robust

observation. However, it remains to be determined whether the expansion of Ly-6G⁺ cells in IL-6^{DC-OE} mice is a direct effect of IL-6. Recently, concerns have been raised as to whether circulating granulocytes can directly respond to IL-6 (22).

Taken together, although we did not aim to dissect direct and indirect effects of IL-6 overexpression in developing devastating inflammation, our data compellingly support the absolute requirement for IL-6R α in mediating IL-6 effects in mice. The fact that our study did not confirm the IL-6–CD5-signaling module proposed for B cells (7) challenges the biological significance of IL-6 signals transduced by an IL-6/CD5/gp130 complex. Our conclusion is in accordance with the recent finding that soluble CD5, despite binding of IL-6, is unable to induce STAT3-mediated signal transduction in gp130-expressing cells (8).

Acknowledgments

We thank the members of the Waisman Laboratory and Bluestone Lab for valuable discussions.

Disclosures

The authors have no financial conflicts of interest.

References

- Kang, S., T. Tanaka, M. Narazaki, and T. Kishimoto. 2019. Targeting interleukin-6 signaling in clinic. *Immunity* 50: 1007–1023.
- Garbers, C., S. Heink, T. Korn, and S. Rose-John. 2018. Interleukin-6: designing specific therapeutics for a complex cytokine. *Nat. Rev. Drug Discov.* 17: 395–412.
- Kamimura, D., K. Ishihara, and T. Hirano. 2003. IL-6 signal transduction and its physiological roles: the signal orchestration model. *Rev. Physiol. Biochem. Pharmacol.* 149: 1–38.
- Babon, J. J., L. N. Varghese, and N. A. Nicola. 2014. Inhibition of IL-6 family cytokines by SOCS3. *Semin. Immunol.* 26: 13–19.
- Rose-John, S., and P. C. Heinrich. 1994. Soluble receptors for cytokines and growth factors: generation and biological function. *Biochem. J.* 300: 281–290.
- Heink, S., N. Yagev, C. Garbers, M. Herwerth, L. Aly, C. Gasperi, V. Husterer, A. L. Croxford, K. Möller-Hackbarth, H. S. Bartsch, et al. 2017. Trans-presentation of IL-6 by dendritic cells is required for the priming of pathogenic T_H17 cells. [Published erratum appears in 2017 *Nat. Immunol.* 18: 474.] *Nat. Immunol.* 18: 74–85.
- Zhang, C., H. Xin, W. Zhang, P. J. Yazaki, Z. Zhang, K. Le, W. Li, H. Lee, L. Kwak, S. Forman, et al. 2016. CD5 binds to interleukin-6 and induces a feed-forward loop with the transcription factor STAT3 in B cells to promote cancer. *Immunity* 44: 913–923.
- Aparicio-Siegmund, S., M. Deseke, A. Lickert, and C. Garbers. 2017. Trans-signaling of interleukin-6 (IL-6) is mediated by the soluble IL-6 receptor, but not by soluble CD5. *Biochem. Biophys. Res. Commun.* 484: 808–812.
- Waage, A., P. Brandtzaeg, A. Halstensen, P. Kierulf, and T. Espevik. 1989. The complex pattern of cytokines in serum from patients with meningococcal septic shock. Association between interleukin 6, interleukin 1, and fatal outcome. *J. Exp. Med.* 169: 333–338.
- Le, R. Q., L. Li, W. Yuan, S. S. Shord, L. Nie, B. A. Habtemariam, D. Przepiorka, A. T. Farrell, and R. Pazdur. 2018. FDA approval summary: tocilizumab for treatment of chimeric antigen receptor T cell-induced severe or life-threatening cytokine release syndrome. *Oncologist* 23: 943–947.
- Wunderlich, F. T., P. Ströhle, A. C. Könnner, S. Gruber, S. Tovar, H. S. Brönneke, L. Juntti-Berggren, L. S. Li, N. van Rooijen, C. Libert, et al. 2010. Interleukin-6 signaling in liver-parenchymal cells suppresses hepatic inflammation and improves systemic insulin action. *Cell Metab.* 12: 237–249.
- Caton, M. L., M. R. Smith-Raska, and B. Reizis. 2007. Notch-RBP-J signaling controls the homeostasis of CD8⁺ dendritic cells in the spleen. *J. Exp. Med.* 204: 1653–1664.
- Haak, S., A. L. Croxford, K. Kreymborg, F. L. Heppner, S. Pouly, B. Becher, and A. Waisman. 2009. IL-17A and IL-17F do not contribute vitally to autoimmune neuro-inflammation in mice. *J. Clin. Invest.* 119: 61–69.
- Peters, M., K. H. Meyer zum Büschenfelde, and S. Rose-John. 1996. The function of the soluble IL-6 receptor in vivo. *Immunol. Lett.* 54: 177–184.
- Jostock, T., J. Müllberg, S. Ozbek, R. Atreya, G. Blinn, N. Voltz, M. Fischer, M. F. Neurath, and S. Rose-John. 2001. Soluble gp130 is the natural inhibitor of soluble interleukin-6 receptor transsignaling responses. *Eur. J. Biochem.* 268: 160–167.
- Abram, C. L., G. L. Roberge, Y. Hu, and C. A. Lowell. 2014. Comparative analysis of the efficiency and specificity of myeloid-Cre deleting strains using ROSA-EYFP reporter mice. *J. Immunol. Methods* 408: 89–100.
- Spencer, S., S. Köstel Bal, W. Egner, H. Lango Allen, S. I. Raza, C. A. Ma, M. Gürel, Y. Zhang, G. Sun, R. A. Sabroe, et al. 2019. Loss of the interleukin-6 receptor causes immunodeficiency, atopy, and abnormal inflammatory responses. *J. Exp. Med.* 216: 1986–1998.
- Van Snick, J., A. Vink, S. Cayphas, and C. Uytendehove. 1987. Interleukin-HP1, a T cell-derived hybridoma growth factor that supports the in vitro growth of murine plasmacytomas. *J. Exp. Med.* 165: 641–649.
- Kantor, A. 1991. A new nomenclature for B cells. *Immunol. Today* 12: 388.
- Ledbetter, J. A., R. V. Rouse, H. S. Micklem, and L. A. Herzenberg. 1980. T cell subsets defined by expression of Lyt-1,2,3 and Thy-1 antigens. Two-parameter immunofluorescence and cytotoxicity analysis with monoclonal antibodies modifies current views. *J. Exp. Med.* 152: 280–295.
- Gorshkova, E. A., R. V. Zvartsev, M. S. Drutska, and E. O. Gubernatorova. 2019. [Humanized mouse models as a tool to study proinflammatory cytokine overexpression]. *Mol. Biol. (Mosk.)* 53: 755–773.
- Wilkinson, A. N., K. H. Gartlan, G. Kelly, L. D. Samson, S. D. Olver, J. Avery, N. Zomerdijs, S. K. Tey, J. S. Lee, S. Vuckovic, and G. R. Hill. 2018. Granulocytes are unresponsive to IL-6 due to an absence of gp130. *J. Immunol.* 200: 3547–3555.

Supplemental materials

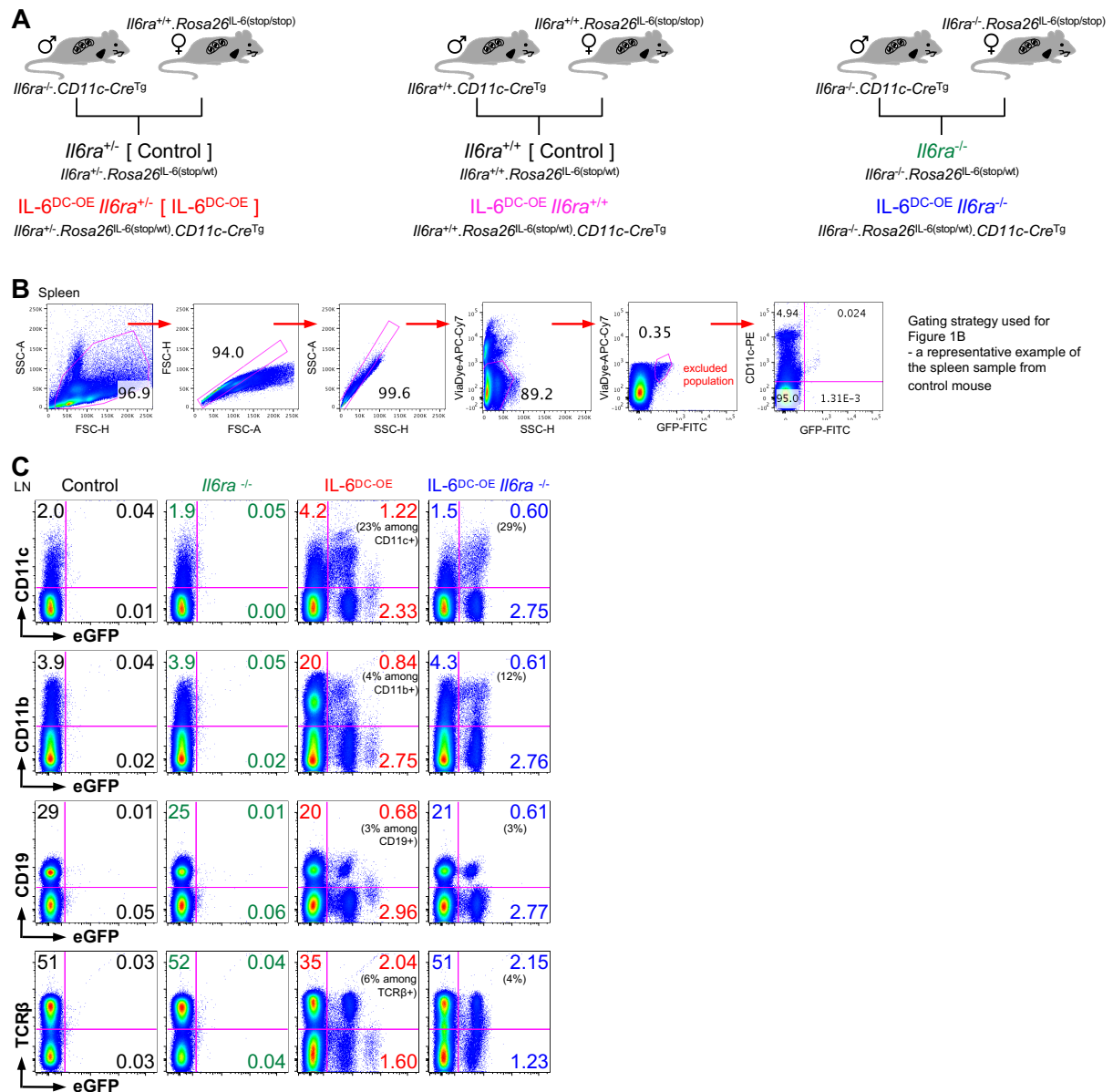
IL-6–Driven Immune Dysregulation Is Strictly Dependent on IL-6R α -Chain Expression

Ilgiz A. Mufazalov, David Andruszewski, Carsten Schelmbauer, Sylvia Heink, Michaela Blanford, Joumana Masri, Yilang Tang, Rebecca Schüler, Christina Eich, F. Thomas Wunderlich, Susanne H. Karbach, Jeffrey A. Bluestone, Thomas Korn and Ari Waisman

Table of Contents

Supplemental Figures 1-3

Supplemental Table I

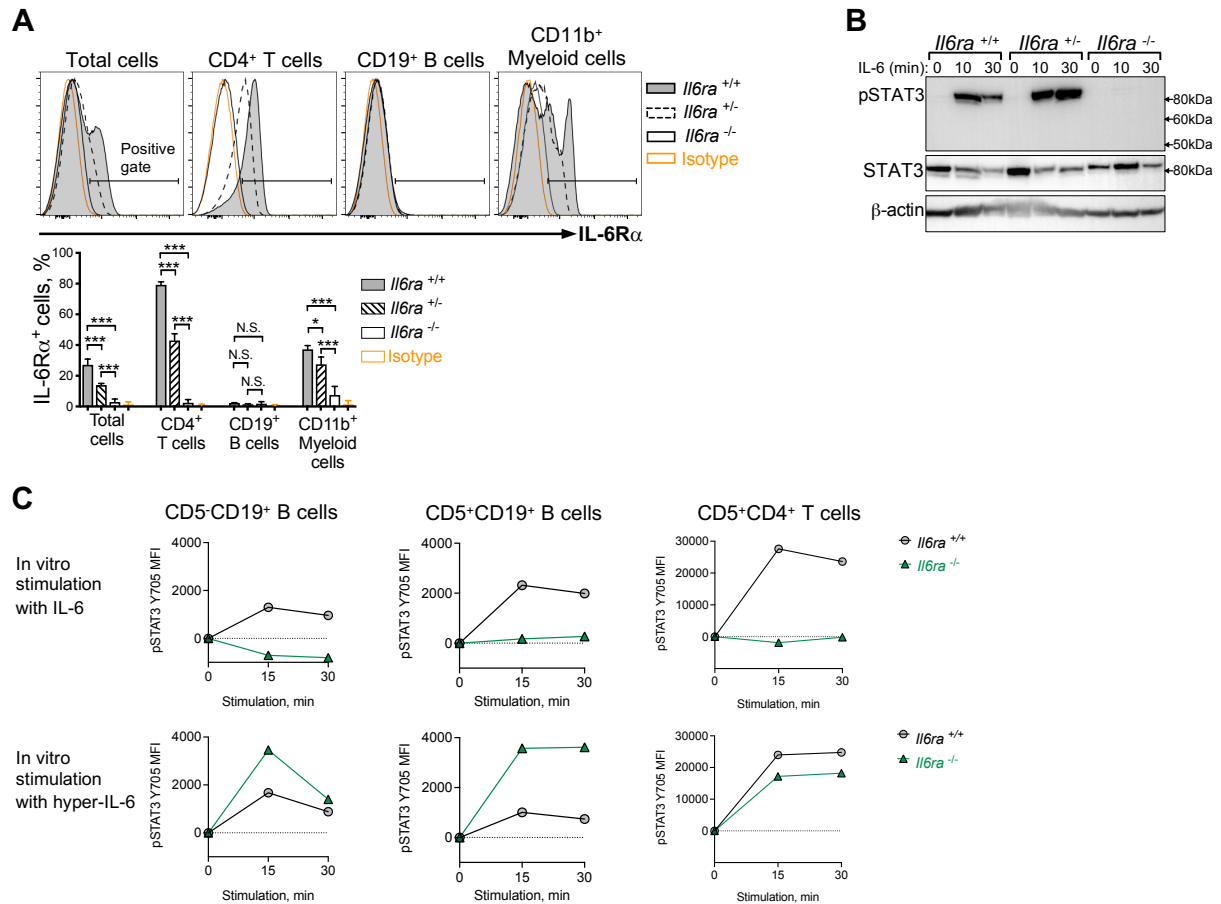


Supplemental Figure 1. Generation and analysis of mice with IL-6 overexpression (Related to Figure 1).

A – Breeding scheme to generate different groups of mice with IL6 overexpression. Tg - transgene; + - wild type (wt) allele; – - knock out allele; DC - dendritic cells; OE - overexpression.

B – Gating strategy used for Figure 1B. After defining VD⁺ live cells autofluorescence in FITC channel was excluded by using “NOT Boolean Gating” FlowJo algorithm.

C – CD11c-Cre-mediated IL-6 overexpression followed by eGFP co-expression across different cell types in lymph nodes. Data depict representative FACS plots with average frequencies per group. Three to five mice per group were used. LN - pooled inguinal, brachial and axillary lymph nodes. All experiments were performed two to three times with similar results.



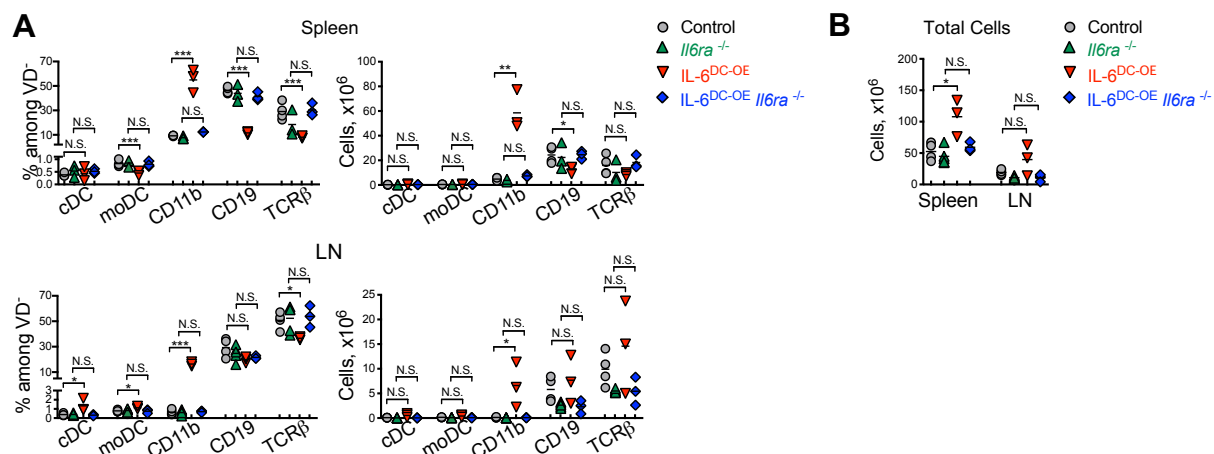
Supplemental Figure 2. Analysis of IL-6 signaling modalities (Related to Figure 1).

A – FACS analysis of IL-6R α expression across different cell types in the spleen. Data depict representative FACS histograms indicating IL-6R α ⁺ cells within the respective parental population. Bar diagram shows mean per group + SD. Isotype control was stained on corresponding cell populations isolated from $Il6ra^{+/+}$ mice. Four mice per group were used. Total cells defined as VD⁻ live cells; CD4⁺ T cells defined as VD⁻CD19⁻TCR β ⁺CD4⁺ cells; CD19⁺ B cells defined as VD⁻TCR β ⁻CD19⁺ cells, CD11b⁺ cells defined as VD⁻CD19⁻TCR β ⁻CD11b⁺ cells.

B – Western blot analysis of STAT3 phosphorylation in total splenocytes in response to IL-6 stimulation *in vitro* (300 ng/ml).

C – FACS analysis of STAT3 phosphorylation in response to *in vitro* stimulation with IL-6 (50 ng/ml) and hyper-IL-6 (125 ng/ml). Mean fluorescence intensity (MFI) of p-STAT3 was normalized to the condition without stimulation (time point 0) per genotype. CD5⁻ and CD5⁺ B cells were isolated from the peritoneal cavity, and CD5⁺CD4⁺ T cells were isolated from the spleen of $Il6ra^{+/+}$ and $Il6ra^{-/-}$ mice, respectively.

*p < 0.05, ***p < 0.001, N.S. – not significant; two-tailed unpaired t-test. All experiments were performed two to three times with similar results.



Supplemental Figure 3. Analysis of different cell types in mice with IL-6 overexpression (Related to Figure 2).

A – Fractions and absolute numbers of different leukocyte subsets in the spleen and lymph nodes of the indicated mouse strains.

B – Cellularity in the spleen and lymph nodes of the indicated mouse strains.

Dot plot graphs (**A-B**) show values for individual mice and mean per group. Three to five mice per group were used. LN - pooled inguinal, brachial and axillary lymph nodes; VD - Viability dye; cDC - conventional dendritic cells, defined as VD⁻CD19⁻TCRβ⁻CD11b⁻CD11c⁺ cells; moDC - myeloid-derived dendritic cells, defined as VD⁻CD19⁻TCRβ⁻CD11b⁺CD11c⁺ cells.

* $p < 0.05$, ** $p < 0.01$, *** $p < 0.001$, N.S. – not significant; two-tailed unpaired t-test. All experiments were performed two to three times with similar results.

Antigen	Clone	Supplier
CD11b	M1/70	Biolegend, eBioscience
CD11c	HL3	BD Biosciences
CD11c	N419	Biolegend
CD19	6D5	Biolegend
CD19	1D3	BD Biosciences
CD23	B3B4	Biolegend
CD4	RM4-5	Biolegend
CD43	S7	BD Biosciences
CD44	IM7	eBioscience
CD45.1	A20	eBioscience
CD45.2	104	Biolegend
CD5	53-7.3	Biolegend
CD62L	MEL-14	eBioscience
CD8	53-6.7	Biolegend
CD90.2	30-H12	Biolegend
CD90.2	53-2.1	Biolegend
F4/80	CI:A3-1	abcam
IgM	II/41	eBioscience
IL-6R α	D7715A7	BD Biosciences
Ly-6C	AL-21	BD Biosciences
Ly-6G	1A8	Biolegend
p-STAT3 (pY705)	4/P-STAT3	BD Biosciences
TCR β	H57-597	Biolegend, BD Biosciences

Streptavidin		Biolegend
--------------	--	-----------

IgG2a, k Isotype	eBR2a	eBioscience
IgG2b, k Isotype	R35-38	BD Biosciences

Viability Dye		eBioscience, 65-0865
Viability Dye		eBioscience, 65-0866

Supplemental Table I. FACS antibodies and viability dyes used in the study.